Bi-directional Evolutionary, Reliability-based, Geometrically Nonlinear, Elasto-Plastic Topology Optimization, of 3D Structures

Muayad Habashneh, Majid Movahedi Rad, Szabolcs Fischer

Széchenyi István University, Egyetem tér 1, Győr 9026, Hungary
e-mail: habashneh.muayad@ hallgato.sze.hu, majidmr@sze.hu, fischersz@sze.hu

Abstract: An extension of bi-directional evolutionary structural optimization, by considering three-dimensional geometrically nonlinear reliability-based elasto-plastic topology optimization, is presented in this study. Due to the important role of the existence of uncertainties to make structural design more practical, this study considers the reliability-based design. Thus, for probabilistic purposes, volume fraction is considered random. The reason of considering the volume fraction as random variable that the application of reliability-based topology optimization shows different topological results comparing to those which are obtained through deterministic designs. By adopting Monte-Carlo technique, the reliability indices are calculated based on the failure probabilities. Different values of volume fractions are considered to explore the effect of changing it on the resultant topologies in case of deterministic design. Furthermore, study the influence of considering different values of reliability indices on the results of probabilistic designs. The plastic-limit analysis is considered in this study in case of elasto-plastic models. A 3D elasto-plastic L-shape beam is considered as a benchmark problem to demonstrate the proficiency of the proposed method. In addition, 3D cantilever beam is considered for deterministic and probabilistic topology optimization designs in cases of elastic and elasto-plastic materials.

Keywords: BESO method; Structural optimization; Geometrically nonlinear analysis; Elasto-plastic deformation; Reliability-based design optimization

Nomenclature

η_{ij}	Total Lagrangian strain	V_i	Element volume
B	Transformation finite element	V^*	Total volume of structure
U	Finite element displacement	V_0	Volume of design domain
s_{ij}	The constituent of second Piola-Kirchhoff stress	V_f	Volume fraction
p_e	Péclet number	N	Number of elements
p	Penalization power	x_i	Binary design variable
C^0_{ijkl}	Solid isotropic material	x	Generated realizations
η_{kl}	The Green-Lagrange strains	X	Random vector
R	Residual vector	$f_X(x)$	Probability joint density

s	Piola-Kirchhoff stress	β	Reliability index
P	The applied load	P_f	Probability of failure
K_T	Tangential stiffness matrix	υ	Poisson's ratio
F_i	Given force	r_{min}	Filter radius
m_s	Load multiplier	ER	Evolutionary volume ratio
F_0	Initial predefined applied forces	τ	Allowable convergence
m_p	Plastic load multiplier	W^c	The complementary work
C	Mean compliance	σ_y	Yield stress
u	Displacement vectors	σ_{HMH}	The Huber-v. Mises-Hencky
K	Global stiffness matrix		

1 Introduction

Topology optimization (TO) is a mathematical approach used to obtain the effectual material distribution within a specified design domain to reach the goal of finding the best structural performance considering fulfilling various constraints. TO has drawn the interest of designers to deal with innovative designs of structures. Thus, the improvement of appropriate applications of (TO) techniques in the construction industry has obtained an increasing consideration [1] [2]. In fact, (TO) can be considered as a promising method to apply in various civil engineering projects such as in concrete and steel structures as well as in case of railway barriers optimization to achieve best designs [3-6]. Besides, (TO) is a powerful technique in finite element analysis of various structures since it allows the designer to identify the parts of the assembly which are unnecessary to satisfy the structure requirements [7-12].

Structural topology optimization has undergone a rapid evolution during last decades. Various tools which facilitate structural optimization in different manners were provided by many authors, for instance, determining load paths in the structures [13], or through determining highly stressed structural areas in a quite effective way [14] [15]. A topology optimization problem of minimizing structural weigh subjected to stress constraints was introduced in the study of Cheng and Jiang [16]. Bi-directional evolutionary structural optimization (BESO) is one of the developed methods which has experienced various improvements recently. In general, the essential idea of (BESO) method is adding and deleting the elements within the design domain at same time according to their sensitivity numbers [17] [18]. A structural topology optimization approach was integrated into laminated composites plates in the study of Chandrasekhar et al. [19] by considering two different goal functions of fundamental frequency and strain energy. Furthermore, Sahithi and Chandrasekhar [20] proposed isogeometric topology optimization based on evolutionary algorithm of swarm intelligence.

Reliability-based topology optimization aims to find a strongly reliable design. Uncertainty topology optimization was considered in the study of Dunning et al. [21] by random assume of the loading magnitude and its direction. Lógó et al. [22] considered uncertainty load condition to develop an updated optimization formulation. Lately, geometrical nonlinearity has been adopted in structural topology optimization by applying it in various problems such as compliant mechanisms and energy absorption. Luo et al. [23] examined in their study topology optimization of structures undergo large displacement. Topology optimization method of elasto-plastic structures was presented in the study of Tauzowski et al. [24]. Blachowski et al. [25] proposed a topology optimization method of elasto-plastic materials considering fulfillment of stress constraints. An updated optimization algorithm considering large displacement was introduced in the study of Gomes and Senne [26]. In the case of materially nonlinear analysis, such as elasto-plastic models, one needs to define the material elastic modulus, plastic hardening and the yield stress to perform elasto-plastic topology optimization. The elastoplastic deformation was considered for topology optimization of composite structures in the study of Kato et al. [27]. Gopal and Panchal [28] proposed an integrated technique to examine the reliability and risk problems within uncertain environment of the process of milk industry.

The three-dimensional topology optimization was considered in various scientific papers. In the study of Liu and Tovar [29], three-dimensional models were considered to perform topology optimization by using MATLAB code. A 3D topology optimization with the aim of minimization of the mean compliance was considered in the study of Zuo and Xie [30]. Langelaar [31] presented a self-supporting topology optimization formulation by considering the effect of excluding unprinted geometries from design domain in case of additive manufacturing.

This study is a continues research work of the development of BESO method, which aims to present 3D reliability-based topology optimization of geometrically nonlinear and elasto-plastic problems. The rest of this paper is organized as following: Section 2 represents theoretical background of the problem. Numerical examples which are considered in this paper are included in Section 3. Finally, the work is summarized in Section 4, the Conclusions.

2 Theoretical Background

2.1 Deterministic Elasto-Plastic BESO

Total nonlinear Lagrangian finite element model is considered to perform the analysis of nonlinear large displacements:

$$\eta_{ij} = \frac{1}{2}\left(u_{i,j} + u_{j,i} + u_{k,i}\, u_{k,j}\right) \tag{1}$$

where u is point-wise displacement, and $i.j$ and k represent coordinate axes.

$$d\eta = B(U)dU \tag{2}$$

where B is the finite element matrix which transforms the change in displacement dU into a strain changing, and U is finite element displacement vector. The Hooke's law for material densities can be expressed as:

$$s_{ij} = (p_e)^p\, C^0_{ijkl}\, \eta_{kl} \tag{3}$$

where s_{ij} is the constituent of second Piola-Kirchhoff stress, p_e represents Péclet number, p is penalization power, C^0_{ijkl} is solid isotropic material constitutive tensor and η_{kl} is the Green-Lagrange strains. Hence, the residual can be defined as the error of the obtained equilibrium.

$$R(U) = P - \int_V B^T \, s \, dV \tag{4}$$

where s refers to the vector of Piola-Kirchhoff stress and P represents the applied load. The equilibrium found when the residual vector equal to zero vector. As a rule, the finite element equilibrium (4) is solved by using Newton-Raphson iterative scheme.

$$K_T = -\frac{\partial R}{\partial U} \tag{5}$$

where $\boldsymbol{K_T}$ is the tangential stiffness matrix.

The plastic-limit analysis is considered in this study in case of elasto-plastic models. The theory of this type of analysis is based on assumption indicates that an elasto-plastic body is exposed to a given force F_i which is gradually increased. The relative load is expressed as:

$$F_i = m_s\, F_0 \tag{6}$$

Where m_s is the load multiplier and F_0 represents the initial predefined applied forces. As m_s increases, plastic zones of the body start to appear until reach extreme intensity which is m_p. Hence, an unrestricted flow of plastic state finally reached. By way of explanation, the corresponding plastic strains and displacements become feasible for the first time during the loading process. According to the definition of plastic limit state, the resultant work of the applied force cannot be negative, therefore, $m_s - m_p \leq 0$.

An extensive explanation of BESO method can be found in various academic papers and literature. Thus, only the applied improvements of BESO method are briefly discussed in this study.

The deterministic elasto-plastic BESO problem can be constructed as following:

$$Minimize: C = u^T K u \tag{7.a}$$

$$Subjected\ to:\ V^* - \sum_{i=1}^{N} V_i x_i = 0 \tag{7.b}$$

$$\frac{V^*}{V_0} - V_f \leq 0 \tag{7.c}$$

$$x_i \in \{0,1\} \tag{7.d}$$

$$m_s - m_p \leq 0 \tag{7.e}$$

Where C stands for the mean compliance, u represents displacement vectors and K denotes the global stiffness matrix. Besides, V_i, V^*, V_0 and V_f represent element volume, total volume of structure, volume of design domain and volume fraction respectively. N is the number of entire elements, and x_i is binary variable which indicates the presence of the solid element. Here, Eq. (7.e) introduces the plastic-limit constraint. Based on the static principle, any statically allowable load multiplier m_s is less or equal the plastic limit load multiplier m_p for the whole design domain.

2.2 Probabilistic Elasto-Plastic BESO

The reliability-based design is considered in this study by applying Monte-Carlo technique. The very basic concept of Monte-Carlo technique is generating of realizations $\boldsymbol{x}$ of the random vector $\boldsymbol{X}$ from their probability joint density function $\boldsymbol{f_X(x)}$. Consequently, the reliability indices $\boldsymbol{\beta}$ is determined by estimating the probability of failure $\boldsymbol{P_f}$ according to the number of the points inside failure domain with respect to the number of total generated points [32]. It should be mentioned that $\boldsymbol{V_f}$ is considered as a random variable having probabilistic characteristics of mean value and standard deviation.

Accordingly, the reliability constraint can be formulated considering the reliability index β as:

$$\beta_{target} - \beta_{calc} \leq 0 \tag{8}$$

where β_{calc} is the calculated reliability index for each iteration and when it reaches the target value of reliability index β_{target}, the program will be terminated since that this constraint is satisfied.

To calculate β_{target} and β_{calc}, the following equations are used:

$$\beta_{target} = -\Phi^{-1}\left(P_{f,target}\right) \tag{9}$$

$$\beta_{calc} = -\Phi^{-1}\left(P_{f,calc}\right) \tag{10}$$

Thus, the probabilistic optimization problem can be illustrated as:

$$Minimize: C = u^T K u \tag{11.a}$$

$$Subject\ to:\ V^* - \sum_{i=1}^{N} V_i x_i = 0 \tag{11.b}$$

$$x_i \in \{0,1\} \tag{11.c}$$

$$m_s - m_p \leq 0 \tag{11.d}$$

$$\beta_{target} - \beta_{calc} \leq 0 \tag{11.e}$$

Here Eqs. (11.a), (11.b) and (11.c) have same roles as Eqs. (7.a), (7.b) and (7.d). While Eq. (7.e) presents the reliability boundary condition on the V_f.

2.3 The Procedure of the Improved BESO

After the brief description of the mathematical technique of the new method, the algorithm can be assembled as shown in Figure 1 for both deterministic and probabilistic designs.

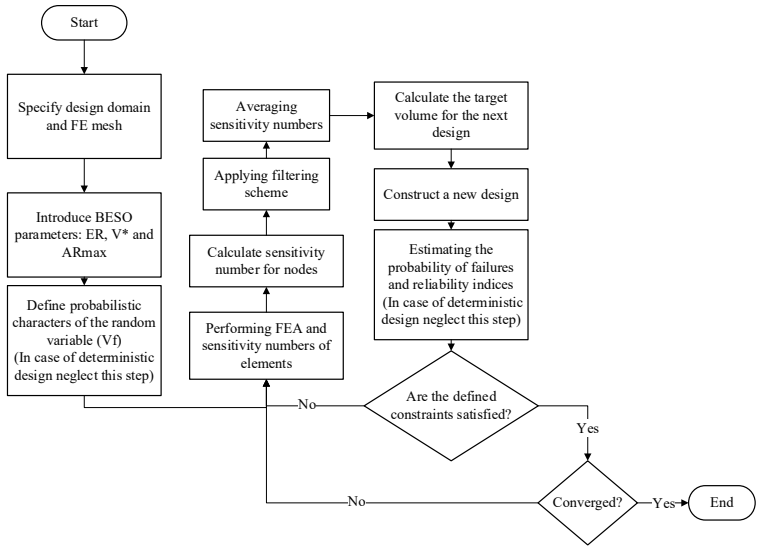

Figure 1
Flow chart of reliability-based geometrically nonlinear elasto-elastic BESO

The algorithm steps can be summed as following:

1) Specify the design domain and FE mesh
2) Introducing BESO parameters
3) Defining mean value and standard deviation (for probabilistic problem)
4) Carrying out finite element simulation
5) Calculate sensitivity numbers for elements and nodes then applying filter and average schemes
6) Calculate the target volume for the next iteration
7) Constructing new design

8) Estimation of the $\boldsymbol{P_f}$ and $\boldsymbol{\beta}$ values (for probabilistic problem)
9) Repeat steps 4-8 until fulfillment of the specified constraints as well as the solution is converged

3 Numerical Examples

In this section, two 3D numerical models are considered for the improved bi-directional evolutionary structural optimization (BESO) method. The first example is a 3D cantilever beam fixed at one end. A 3D L-shape beam model is considered as the second example, to demonstrates the efficiency of the proposed method, the results of this example are compared with a benchmark example which was done by Rad et al. [33]. For purpose of evaluating probabilistic nature, Monte-Carlo technique as well as V_f is considered as random variable with mean value and standard deviation.

3.1 3D Cantilever Beam Model

The first example in this study is 3D cantilever model. At the beginning, reliability-based topology optimization of elastic linear and geometrically nonlinear models is considered. Then, reliability elasto-plastic topology optimization is considered for the same model. The design domain of the model is represented in Figure 2. The common parameters for both optimization processes are Young's modulus of $70.2\ GPa$ with Poisson's ratio $\upsilon = 0.25$. BESO parameters are $r_{min} = 3\ mm$, $ER = 3\%$, and $\tau = 0.1\%$. In addition, volume fraction V_f is assumed random and has probabilistic properties of mean value 10% and standard deviation 5%. Finally, Monte-Carlo technique is considered with number of simulations 3.0×10^6.

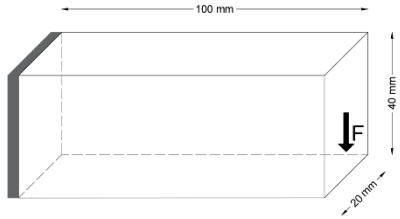

Figure 2
3D cantilever beam model

3.1.1 Elastic Topology Optimization Problem

Elastic reliability-based topology optimization of linear and geometrically nonlinear models is considered in this part. Considering that the applied load at the free end as shown in Figure 2 has a magnitude of $F = 1\ kN$.

The resulted topological designs of linear and geometrically nonlinear analysis beside the complementary work W^c of different volume fraction values of deterministic design are shown in Table 1. It can be noted from Table 1 that there is a significant decrease in the complementary work from linear design to geometrically nonlinear designs for each value of volume fraction. By considering $V_f = 0.16$, the complementary work value dropped down by 22.2% from 1.35 kJ in linear case to 1.05 kJ in geometrically nonlinear case. Also, for $V_f = 0.10$, the complementary work value declined by 37.3% from 1.93 kJ in linear case to 1.21 kJ in geometrically nonlinear design. Thus, the optimal resulted topologies in case of nonlinear designs are stiffer than those which are obtained in case of linear design. Besides, according to the obtained results, it should be mentioned that as V_f declines the complementary work raises for elastic linear and geometrically nonlinear models.

Table 1
Resulted topological designs and complementary work in case of deterministic design

	V_f	Optimized shape	W^c		V_f	Optimized shape	W^c
Deterministic linear designs from BESO	0.16	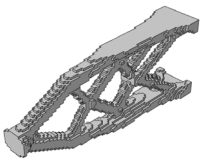	1.35	Deterministic geometrically nonlinear designs from BESO	0.16	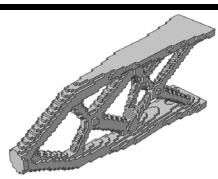	1.05
	0.12	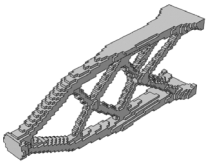	1.72		0.12	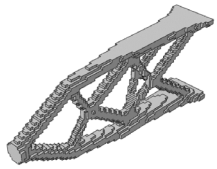	1.13
	0.10	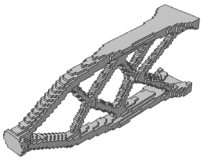	1.93		0.10	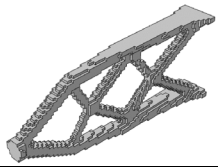	1.21

Table 2 shows the resulted topological designs of probabilistic linear and geometrically nonlinear analysis beside the complementary work W^c considering different β_{target} values. It can be noted that there are significant differences in the complementary work between linear design and geometrically nonlinear designs for each case of volume fraction. By considering $\beta_{target} = 4.37$, the complementary work value dropped by 13.01% from 1.69 kJ in linear case to 1.47 kJ in geometrically nonlinear case. In addition, for the lowest value of target reliability index $\beta_{target} = 3.05$, the complementary work value fallen by 10.28% from 1.75 kJ in linear case to 1.57 kJ in geometrically nonlinear design. In other words,

in case of geometrically nonlinear designs, the resulted topologies are stiffer from which are obtained in case of linear designs. Also, it can be said that as β_{target} become less the complementary work raises for elastic linear and geometrically nonlinear models.

Table 2
Resulted topological designs and complementary work in case of probabilistic design

	β_{target}	Optimized shape	W^c		β_{target}	Optimized shape	W^c
Probabilistic linear designs from BESO	4.37	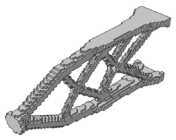	1.69	Probabilistic geometrically nonlinear designs from BESO	4.37	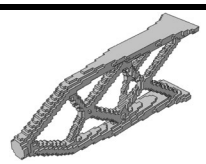	1.47
	3.64	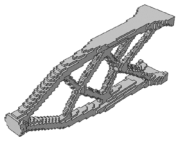	1.71		3.64	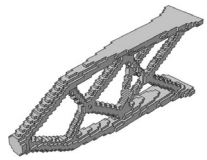	1.52
	3.05	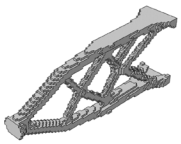	1.75		3.05	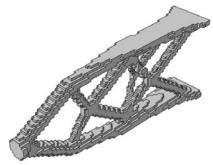	1.57

3.1.2 Elasto-Plastic Topology Optimization Problem

Deterministic and probabilistic geometrically nonlinear topology optimizations of elasto-plastic 3D cantilever model are considered in this part. The yield stress equals $\sigma_y = 135\ MPa$. The plastic-limit load multiplier m_p is assumed 5.0, the initial load is assumed to be $F_0 = 0.5\ kN$ and the ultimate load is $F_{\text{ult}} = 2.6\ kN$. To demonstrate the effect of load multiplier, three load cases are considered: $F_1 = 0.5\ F_0$, $F_2 = 2.5\ F_0$, $F_3 = 5\ F_0$.

Table 3 represents the Huber-v. Mises-Hencky (HMH) stresses of deterministic resulted topological optimum designs of geometrically nonlinear analysis for different values of V_f considering three different values of load multiplier F_1, F_2 and F_3.

According to the results which are included in Table 3, it can be noticed that in case of lowest applied load ($F_1 = 0.5\ F_0$), the mean stress is increased by 18.27% from $10.96\ MPa$ in case of $V_f = 0.16$ to $13.41\ MPa$ when $V_f = 0.10$. Corresponding to the highest load multiplier ($F_3 = 5.0\ F_0$), the mean stress is raised by 10.37% from $90.36\ MPa$ in case of $V_f = 0.16$ to $100.81\ MPa$ when $V_f = 0.10$. Thus, according to these results, we can say that as V_f decreases, that the mean stress increases for each loading case.

Table 3
Resulted topological designs and HMH stresses according to various V_f considering F_1, F_2 *and* F_3

V_f	$F_1 = 0.5\,F_0$ $\frac{\sigma_{HMH}}{\sigma_y}$	$F_2 = 2.5\,F_0$ $\frac{\sigma_{HMH}}{\sigma_y}$	$F_3 = 5.0\,F_0$ $\frac{\sigma_{HMH}}{\sigma_y}$
0.16	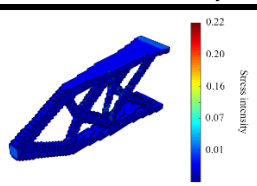	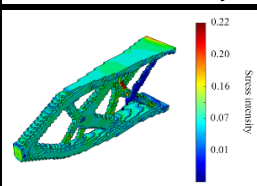	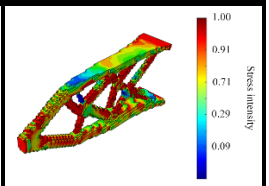
Mean stress (MPa)	10.96	54.41	90.36
0.12	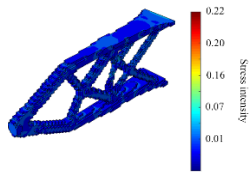	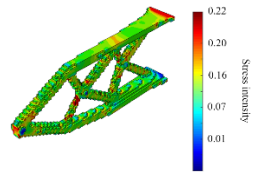	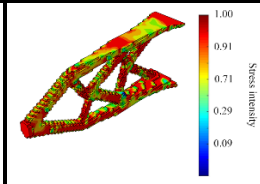
Mean stress (MPa)	11.26	55.68	96.92
0.10	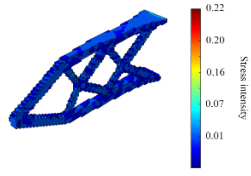	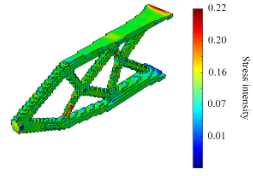	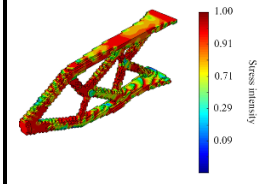
Mean stress (MPa)	13.41	67.05	100.81

Furthermore, it can be observed from the obtained results that in case of first load multiplier there is almost no plastic regions. While, in case of highest load multiplier, plastic zones are obtained largely.

The corresponding Huber-v. Mises-Hencky (HMH) stresses of different load cases $F_1 = 0.5\,F_0$, $F_2 = 2.5\,F_0$ and $F_3 = 5\,F_0$ according to the resulted probabilistic geometrically nonlinear topological designs are shown in Table 4. Considering that three values of β_{target} are considered.

According to Table 4, it is well noticed that in case of lowest load case ($F_1 = 0.5\,F_0$), the mean stress is increased by 6.20% from $10.74\,MPa$ in case of $\beta_{target} = 4.37$ to $11.45\,MPa$ when $\beta_{target} = 3.05$. Corresponding to the highest load multiplier ($F_3 = 3.05\,F_0$), the mean stress is raised by 5.92% from $89.77\,MPa$ in case of $\beta_{target} = 4.37$ to $95.42\,MPa$ when $\beta_{target} = 3.05$.

Table 4
Resulted topological designs and HMH stresses according to various β_{target} considering F_1, F_2 and F_3

β_{target}	$F_1 = 0.5\ F_0$ $\frac{\sigma_{HMH}}{\sigma_y}$	$F_2 = 2.5\ F_0$ $\frac{\sigma_{HMH}}{\sigma_y}$	$F_3 = 5.0\ F_0$ $\frac{\sigma_{HMH}}{\sigma_y}$
4.37	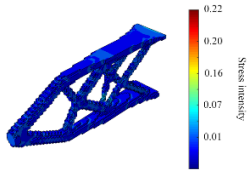	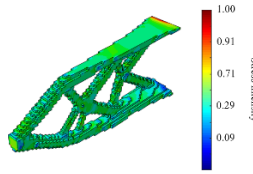	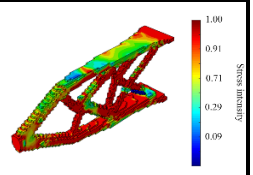
Mean stress (MPa)	10.74	53.72	89.77
3.64	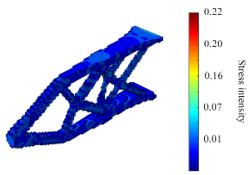	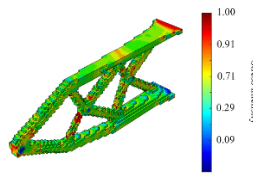	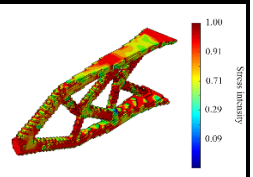
Mean stress (MPa)	11.08	55.56	92.20
3.05	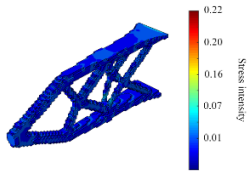	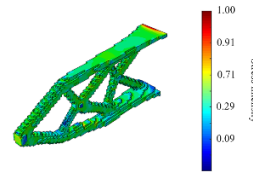	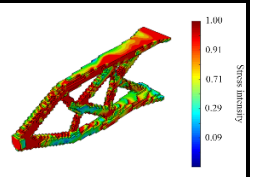
Mean stress (MPa)	11.45	57.32	95.42

In other words, the mean stress increases as β_{target} decreases for each loading case. Also, the effect of load multiplier can be observed from the obtained results since that in the case of first load multiplier there is almost no plastic regions. While, in case of the highest load multiplier, plastic zones are obtained largely.

3.2 3D L-Shape Beam Model

3D L-shape model is the considered as the second example in this study. Figure 3 represents the design domain of this problem. This work has implemented deterministic and probabilistic geometrically nonlinear elasto-plastic topology optimization. An applied load F is acting at the top of the free end. Material properties are assumed 200 GPa of Young's modulus and 0.25 of Poisson's ratio. Considering that BESO parameters are $r_{min} = 18mm$, $ER = 1\%$, and $\tau = 0.1\%$.

Volume fraction V_f has the probabilistic properties of mean value 21% and standard deviation 5%. The number of Monte-Carlo simulation is assumed 3.0×10^6.

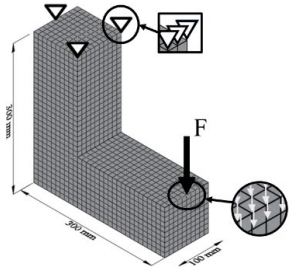

Figure 3
3D L-shaped beam model

For purposes of considering plastic-limit analysis, the initial load is assumed $F_0 = 10\ kN$ and the value of yield stress $\sigma_y = 93\ Mpa$. In addition, the limit of plastic load is $m_p = 3.48$. consequently, four load cases are considered in this problem: $F_1 = 0.348F_0$, $F_2 = 2.262F_0$, $F_3 = 3.30F_0$. Finally, as mentioned previously, the results of this work are compared with the study of Rad et al. [33]. Similar to the previous problem, Table 5 shows the results of deterministic topological optimum designs of elasto-plastic geometrically nonlinear analysis for different values of V_f according to $F_1 = 0.348F_0$, $F_2 = 2.262F_0$ and $F_3 = 3.30F_0$.

Table 5
Resulted topological designs and HMH stresses according to various V_f by considering F_1, F_2 *and* F_3

V_f	$F_1 = 0.348F_0$ $\frac{\sigma_{HMH}}{\sigma_y}$	$F_2 = 2.262F_0$ $\frac{\sigma_{HMH}}{\sigma_y}$	$F_3 = 3.30F_0$ $\frac{\sigma_{HMH}}{\sigma_y}$
0.30	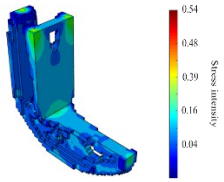	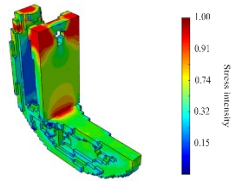	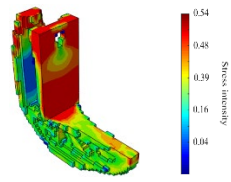
Mean stress (MPa)	6.71	45.41	60.21
0.28	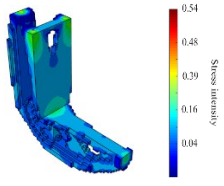	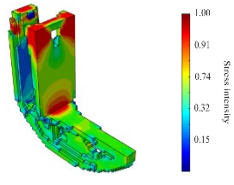	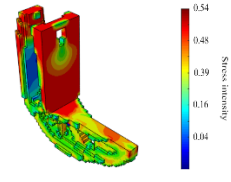
Mean stress (MPa)	7.19	48.63	64.67

0.27	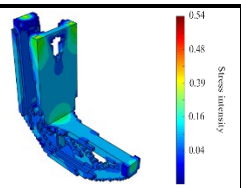	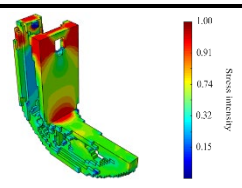	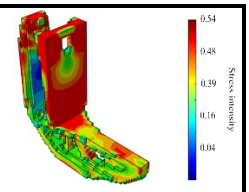
Mean stress (MPa)	7.48	50.65	67.50

Similarly, to the results of previous problem, it can be noticed that the mean stress increases as V_f decreases for each loading case. As obtained from the results of lowest load case ($F_1 = 0.348\,F_0$), the mean stress is increased by 10.29% from $6.71\ MPa$ in case of $V_f = 0.30$ to $7.48\ MPa$ when $V_f = 0.27$. Also, for the highest load multiplier ($F_3 = 3.30\,F_0$), the mean stress is increased by 10.80% from $60.21\ MPa$ in case of $V_f = 0.30$ to $67.50\ MPa$ when $V_f = 0.27$. Besides, here again the significant effect of load multiplier can be noticed from the obtained results since that in the case of first load multiplier there is almost no plastic regions. While the plastic zones are obtained largely in case of the highest load multiplier. Table 6 represents the corresponding Huber-v. Mises-Hencky (HMH) stresses of load multiplier $F_1 = 0.348\,F_0$, $F_2 = 2.262\,F_0$ and $F_3 = 3.30\,F_0$ in case of probabilistic elasto-plastic geometrically nonlinear topological designs. By considering three different values of β_{target}.

Table 6
Resulted topological designs and HMH stresses according to various β_{target} by considering F_1, F_2 and F_3

β_{target}	$F_1 = 0.348F_0$ $\frac{\sigma_{HMH}}{\sigma_y}$	$F_2 = 2.262F_0$ $\frac{\sigma_{HMH}}{\sigma_y}$	$F_3 = 3.30F_0$ $\frac{\sigma_{HMH}}{\sigma_y}$
4.97	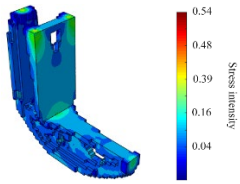	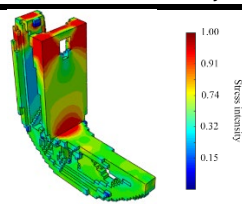	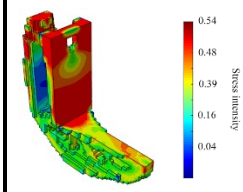
Mean stress (MPa)	6.04	44.63	60.03
4.16	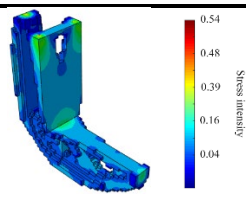	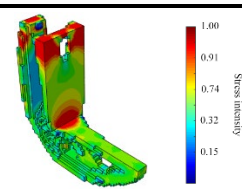	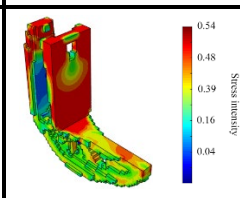
Mean stress (MPa)	6.87	46.34	63.70

3.21	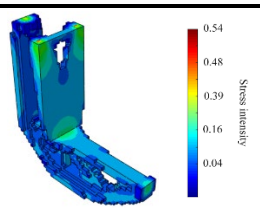	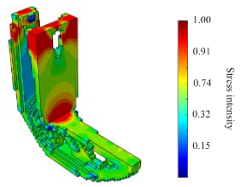	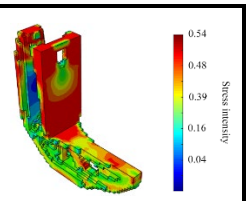
Mean stress (MPa)	7.15	49.72	66.20

Table 6 shows that the increasing percentage of the mean stress is 15.52% from 6.04 MPa in case of $\beta_{target} = 4.97$ to 7.15 MPa when $\beta_{target} = 3.21$ according to the lowest load case ($F_1 = 0.348\ F_0$). Also, 9.32% is the increasing percentage of the mean stress from 60.03 MPa in case of $\beta_{target} = 4.97$ to 66.20 MPa in case of $\beta_{target} = 3.21$ according to the highest load case ($F_3 = 3.30\ F_0$). Thus, we can say that the mean stress increases as β_{target} decreases for each loading case. Again, here we can notice that in the case of first load multiplier there is no obtained plastic zones. On the other hand, by increasing the applied load, plastic zones can be obtained sufficiently until reach the plastic-limit load.

Conclusions

This work concerns the expansion of a reliability-based, geometrically nonlinear, elasto-elastic topology optimization, of 3D structures, by considering an extended BESO method. Due to the existence of uncertainties, V_f is treated as a random variable during the optimization process. The reliability-based design is performed, by adopting Monte-Carlo simulation method, by determining the reliability indices according to the values of failure probabilities. In the case of elasto-plastic structures, the plastic-limit analysis method is considered. The proposed method can be considered as an effective structural optimization method, for solving the three-dimensional design problems, associated with a goal of mean compliance minimization. The results of the benchmark problem, obviously validate the efficiency of the proposed method.

The work done in this study, can be summarized, by the following points:

1) In case of deterministic design, when multiple $\boldsymbol{V_f}$ values are considered, there is a negative correlation between $\boldsymbol{V_f}$ and complementary work. Also, between $\boldsymbol{V_f}$ and the values of mean stresses.
2) In case of Probabilistic design, when multiple values of $\boldsymbol{\beta_{target}}$ are considered, it can be noted that as $\boldsymbol{\beta_{target}}$ decreases, the complementary work and the values of mean stresses increase.
3) For both deterministic and probabilistic designs, the complementary work values of geometrically nonlinear designs are smaller than which obtained in case of linear designs.

4) It is noted, that in elasto-plastic design for both deterministic and probabilistic cases, there is almost no plastic regions obtained corresponding to the lowest acting load, while the plastic zones are clearly visible in case of highest acting load.

This paper can be considered as a huge improvement, towards a more sensible and more extensive framework, for three-dimensional geometrically nonlinear elastic and elasto-plastic topology optimization, by adopting the plastic-limit analysis considering reliability constraint. Thus, based on the noted examples, the proposed approach can be considered as a valuable work in the work associated with finding the optimal topologies, in the design of structures, as compared to other methods. The proposed BESO method has the fundamental advantages of the basic BESO algorithm, exactly, effectiveness and simplicity. In addition, according to the obtained results, we can say that the optimum solutions are firmer in the case of geometrically nonlinear designs, than in the case of linear designs. However, the main concern of the proposed model is related to the global optimum. Thus, it is herein recommended to validate the loading and boundary conditions for each iteration. Nonetheless, additional research is planned to include other nonlinear designs.

References

[1] Błachowski B, Świercz A, Ostrowski M, Tauzowski P, Olaszek P, Jankowski Ł. Convex relaxation for efficient sensor layout optimization in large-scale structures subjected to moving loads. Computer-Aided Civil and Infrastructure Engineering 2020;35:1085–100. https://doi.org/10.1111/mice.12553.

[2] Duysinx P, Bendsøe MP. Topology optimization of continuum structures with local stress constraints. International Journal for Numerical Methods in Engineering 1998;43:1453–78. https://doi.org/10.1002/(SICI)1097-0207(19981230)43:8<1453::AID-NME480>3.0.CO;2-2.

[3] Kurhan D, Kurhan M, Husak M. Impact of the variable stiffness section on the conditions of track and rolling stock interaction. IOP Conference Series: Materials Science and Engineering, vol. 985, 2020, p. 12005. https://doi.org/10.1088/1757-899X/985/1/012005.

[4] Kurhan M, Kurhan D, Novik R, Baydak S, Hmelevska N. Improvement of the railway track efficiency by minimizing the rail wear in curves. IOP Conference Series: Materials Science and Engineering, vol. 985, 2020, p. 12001. https://doi.org/10.1088/1757-899X/985/1/012001.

[5] Mahmood T, Haleemzai I, Ali Z, Pamucar D, Marinkovic D. Power Muirhead Mean Operators for Interval-Valued Linear Diophantine Fuzzy Sets and Their Application in Decision-Making Strategies. Mathematics 2022;10:70. https://doi.org/10.3390/math10010070.

[6] Kuchak AJT, Marinkovic D, Zehn M. Parametric Investigation of a Rail Damper Design Based on a Lab-Scaled Model. Journal of Vibration Engineering & Technologies 2021;9:51–60. https://doi.org/10.1007/s42417-020-00209-2.

[7] He CH, Liu C, He JH, Mohammad-Sedighi H, Shokri A, Gepreel KA. A fractal model for the internal temperature response of a porous concrete. Appl Comput Math 2021;20. https://doi.org/10.1016/j.ijheatmasstransfer.2018.09.072.

[8] Saberi Varzaneh A, Naderi M. Experimental and Finite Element Study to Determine the Mechanical Properties and Bond Between Repair Mortars and Concrete Substrates. Journal of Applied and Computational Mechanics 2022;8:493–509. https://doi.org/10.22055/jacm.2020.32921.2101.

[9] Di Re P, Addessi D. Computational Enhancement of a Mixed 3D Beam Finite Element with Warping and Damage. Journal of Applied and Computational Mechanics 2022;8:260–81. https://doi.org/10.22055/jacm.2021.37948.3120.

[10] Pavlovic A, Fragassa F. Geometry optimization by fem simulation of the automatic changing gear. Reports in Mechanical Engineering 2020;1:199–205. https://doi.org/10.31181/rme200101199p.

[11] Wu F, Wang Z, Song D, Lian H. Lightweight design of control arm combining load path analysis and biological characteristics. Reports in Mechanical Engineering 2022;3:71–82. https://doi.org/10.31181/rme2001210122w.

[12] Fragassa C. Lightening structures by metal replacement: from traditional gym equipment to an advanced fiber-reinforced composite exoskeleton. Facta Universitatis, Series: Mechanical Engineering 2021;19:155–74. https://doi.org/10.22190/FUME201215043F.

[13] Zhao S, Mao L, Wu N, Karnaoukh S. LOAD PATH VISUALIZATION USING U* INDEX AND PRINCIPAL LOAD PATH DETERMINATION IN THIN-WALLED STRUCTURES. Facta Universitatis, Series: Mechanical Engineering 2022;0.

[14] Strzalka C, Manfred Z. The influence of loading position in a priori high stress detection using mode superposition. Reports in Mechanical Engineering 2020;1:93–102. https://doi.org/10.31181/rme200101093s.

[15] Strzalka C, Marinkovic D, Zehn MW. Stress Mode Superposition for a Priori Detection of Highly Stressed Areas: Mode Normalisation and Loading Influence. Journal of Applied and Computational Mechanics 2021;7:1698–709. https://doi.org/10.22055/jacm.2021.36637.2878.

[16] CHENG G, JIANG Z. STUDY ON TOPOLOGY OPTIMIZATION WITH STRESS CONSTRAINTS. Engineering Optimization 1992;20:129–48. https://doi.org/10.1080/03052159208941276.

[17] Li Y, Huang XD, Xie YM, Zhou SW. Bi-Directional Evolutionary Structural Optimization for Design of Compliant Mechanisms. Advances in Engineering Plasticity XI, vol. 535, Trans Tech Publications Ltd; 2013, p. 373–6. https://doi.org/10.4028/www.scientific.net/KEM.535-536.373.

[18] Radman A. Combination of BESO and harmony search for topology optimization of microstructures for materials. Applied Mathematical Modelling 2021;90:650–61. https://doi.org/10.1016/j.apm.2020.09.024.

[19] Chandrasekhar KN v, Bhikshma V, Bhaskara Reddy KU. Topology Optimization of Laminated Composite Plates and Shells using Optimality Criteria. Journal of Applied and Computational Mechanics 2022;8:405–15. https://doi.org/10.22055/jacm.2019.31296.1858.

[20] Sahithi NSS, Chandrasekhar KN v. Isogeometric Topology Optimization of Continuum Structures using an Evolutionary Algorithm. Journal of Applied and Computational Mechanics 2019;5:414–40. https://doi.org/10.22055/jacm.2018.26398.1330.

[21] Dunning PD, Kim HA, Mullineux G. Introducing loading uncertainty in topology optimization. AIAA Journal 2011;49:760–8. https://doi.org/10.2514/1.J050670.

[22] Lógó J, Ghaemi M, Rad MM. Optimal topologies in case of probabilistic loading: the influence of load correlation. Mechanics Based Design of Structures and Machines 2009;37:327–48. https://doi.org/10.1080/15397730902936328.

[23] Luo Y, Wang MY, Kang Z. Topology optimization of geometrically nonlinear structures based on an additive hyperelasticity technique. Computer Methods in Applied Mechanics and Engineering 2015;286:422–41.

[24] Tauzowski P, Blachowski B, Lógó J. Topology optimization of elasto-plastic structures under reliability constraints: A first order approach. Computers & Structures 2021;243:106406. https://doi.org/10.1016/j.compstruc.2020.106406.

[25] Blachowski B, Tauzowski P, Lógó J. Yield limited optimal topology design of elastoplastic structures. Structural and Multidisciplinary Optimization 2020:1–24. https://doi.org/10.1007/s00158-019-02447-9.

[26] Gomes FAM, Senne TA. An algorithm for the topology optimization of geometrically nonlinear structures. International Journal for Numerical Methods in Engineering 2014;99:391–409. https://doi.org/10.1002/nme.4686.

[27] Kato J, Hoshiba H, Takase S, Terada K, Kyoya T. Analytical sensitivity in topology optimization for elastoplastic composites. Structural and Multidisciplinary Optimization 2015;52:507–26. https://doi.org/10.1007/s00158-015-1246-8.

[28] Gopal N, Panchal D. A STRUCTURED FRAMEWORK FOR RELIABILITY AND RISK EVALUATION IN THE MILK PROCESS INDUSTRY UNDER FUZZY ENVIRONMENT. Facta Universitatis, Series: Mechanical Engineering 2021;19:307–33. https://doi.org/10.22190/FUME201123004G.

[29] Liu K, Tovar A. An efficient 3D topology optimization code written in Matlab. Structural and Multidisciplinary Optimization 2014;50:1175–96. https://doi.org/10.1007/s00158-014-1107-x.

[30] Zuo ZH, Xie YM. A simple and compact Python code for complex 3D topology optimization. Advances in Engineering Software 2015;85:1–11. https://doi.org/https://doi.org/10.1016/j.advengsoft.2015.02.006.

[31] Langelaar M. Topology optimization of 3D self-supporting structures for additive manufacturing. Additive Manufacturing 2016;12:60–70. https://doi.org/https://doi.org/10.1016/j.addma.2016.06.010.

[32] Stanton A, Wiegand D, Stanton G. Probability reliability and statistical methods in engineering design 2000.

[33] Rad MM, Habashneh M, Lógó J. Elasto-Plastic limit analysis of reliability based geometrically nonlinear bi-directional evolutionary topology optimization. Structures, vol. 34, 2021, p. 1720–33. https://doi.org/10.1016/j.istruc.2021.08.105.